Journal of Solid State Chemistry 188 (2012) 105–108

Contents lists available at SciVerse ScienceDirect

Journal of Solid State Chemistry

journal homepage: www.elsevier.com/locate/jssc

Luminescence of the elpasolite series $M^I_2M^{II}MCl_6$ (M^I=Cs, Rb; M^{II}=Li, Na; M=Lu, Y, Sc, In) doped with europium using synchrotron radiation excitation

Peter A. Tanner [a,*], Chang-Kui Duan [b], Guohua Jia [c], Bing-Ming Cheng [d]

[a] Faculty of Physics and Optoelectronic Engineering, Guangdong University of Technology, Guangzhou 510006, PR China
[b] Department of Physics, University of Science and Technology of China, Hefei, Anhui, PR China
[c] College of Materials Science and Engineering, China Jiliang University, Hangzhou 310018, PR China
[d] National Synchrotron Radiation Research Center, Hsinchu, Taiwan

ARTICLE INFO

Article history:
Received 19 October 2011
Received in revised form
17 January 2012
Accepted 23 January 2012
Available online 5 February 2012

Keywords:
Divalent europium
Trivalent europium
Ultraviolet emission
Elpasolite lattice
Synchrotron radiation

ABSTRACT

The excitation and emission spectra of a series of cubic hexachloroelpasolites doped with europium have been investigated using synchrotron radiation at 10 K. Besides the Eu^{3+} emission from ^5D_J (J=0–3) multiplets, emission from $^5H_3$ is also observed for $Cs_2NaIn_{0.995}Eu_{0.005}Cl_6$, since the gap to the next lowest level is spanned by seven phonons. The excitation spectra of samples indicate impurities due to oxygen and divalent europium. Broad band emission from Eu^{2+} is reported from the crystalline samples grown in vacuum by the Bridgman process, with the maximum wavelength shifting to the red with increasing lattice parameter for the series Cs_2NaMCl_6:Eu^{2+} (M=Lu, Y, Eu).

1. Introduction

We have recently reported the excitation and emission spectra of pure and doped hexachloroelpasolite systems, $Cs_2NaLnCl_6$ (Ln=Y, Nd, Sm, Eu, Gd, Tb, Er, Yb) and Cs_2NaYCl_6:Ln^{3+} (Ln=Ce, Sm, Er, Tm) excited by synchrotron radiation [1,2]. The focus of these studies was the simulation of the $4f^N \rightarrow 4f^{N-1}5d$ absorption spectra and the comparison with the observed excitation spectrum. The major result was the description of the states of the Ln^{3+} $4f^N$, Ln^{3+} $4f^{N-1}5d$, and Ln^{2+} $4f^{N+1}$ configurations relative to the valence and conduction bands of $Cs_2NaLnCl_6$, for which the band gaps are between 6.6 and 8.1 eV [2]. No $4f^{N-1}5d \rightarrow 4f^N$ emission was observed for these systems, with the exceptions of Ln=Ce, Pr [3,4]. However, for all of these systems (except Ln=Y, Ce), well-resolved $4f^N \rightarrow 4f^N$ luminescence was observed and assigned. The absence of $4f^{N-1}5d \rightarrow 4f^N$ emission contrasts with the behaviour of other systems, such as YPO_4 [5], $LiYF_4$ [5,6], M_3LnF_6 [7], and other wide-band gap fluorides [8], where fast interconfigurational emission has been observed for most lanthanide ions, except for Ln=Y, Pm, Tb, Yb systems.

There are many reasons why broad emission bands appear in the vacuum ultraviolet (VUV) and ultraviolet (UV) spectra of Ln^{3+}-doped into insulators and the excitation mechanisms [9–11] and processes connected with luminescence [12,13] have been reviewed. In particular, much attention has focused upon the luminescence of cubic alkali halide crystals at low temperature and the nature of self-trapped excitons [14–16]. The self-trapped exciton (the V_k^- centre: isoelectronic with a $(\text{halogen})_2^{2-}$ ion), in alkali halide crystals exhibits emission bands at 370 nm (NaCl) and 536 nm (KCl), which are quenched above 50–100 K [14]. The elpasolites also exhibit cubic crystal structures, with Na^+ and Y^{3+} ions in Cs_2NaYCl_6 forming a sublattice of NaCl structure. The investigation of radiation-induced defects in Cs_2NaYF_6 showed the presence of V_K, H_A-type, and Y^{2+} centres [17,18]. Dorenbos and van Eijk have published many papers concerning the "anomalous" luminescence of Ce^{3+} in elpasolite host lattices [19–25]. The hexachloroelpasolites are deliquescent so that substitution of Cl by O or OH readily occurs. Absorption bands due to various oxygen centres: O^- (at 225 nm [26]), O_2^{2-} (260 nm [27]), O_2^- (215 nm [27], 244 nm [28]), O^{2-} (286, 440 nm [28]) have previously been reported for other systems. The excitation spectrum of the broad emission band at 368 nm at 300 K for a sample of $Cs_2NaEuCl_6$ showed an intense feature at 248 nm [2], which was associated with Eu–O charge transfer (CT) absorption [2,29]. The CT absorption is a two-centre process:

$$Eu^{3+}(\text{g.s.}) + VB(e^-) \rightarrow Eu^{2+}(\text{e.s.}) + VB(\text{hole})$$

where g.s. and e.s. refer to ground and excited vibrational states; VB refers to the valence band, mainly comprising oxygen 2p electrons in this case. Although Eu–Cl CT bands have previously been assigned in excitation [2,30] and absorption [31]

* Corresponding author.
E-mail address: peter.a.tanner@gmail.com (P.A. Tanner).

0022-4596/$ - see front matter © 2012 Elsevier Inc. All rights reserved.
doi:10.1016/j.jssc.2012.01.047

spectra, we are unaware of conclusive assignments of the corresponding emission bands. In fact, van Pieterson et al. [30] have stated that Eu^{3+} CT emission is not observed due to fast relaxation to ^5D_J states. Finally, ultraviolet emission bands may be due to 5d→4f transitions of a trace impurity of Ce^{3+} [4], Pr^{3+} [3], or Eu^{2+} [32]. For the latter, the one-centre transition is:

Eu^{2+} ($4f^6 5d^1$ T_{2g})→Eu^{2+} ($^8S_{7/2}$ $4f^7$, vibrationally excited).

In this study we have investigated some of the broad spectral features that are present in the excitation and emission spectra of lanthanide hexachloroelpasolites doped with europium, using synchrotron radiation excitation and we make comments concerning the nature of these bands.

2. Experimental

2.1. Materials

Chemicals LiCl (99.9%), RbCl (99.9%), NaCl (99.999%), CsCl (99.999%), Eu_2O_3 (99.999%), and R_2O_3 (99.999%, R=Sc, Lu, Y or In) were purchased from Strem and used as received without further purification. Cs_2NaRCl_6:Eu^{3+} were prepared according to the method E of Morss et al. [33], using a 5% stoichiometric excess of the chlorides. In a beaker, the oxide was dissolved in concentrated HCl (Aristar, Riedel-de-Hähn) with heating. Then the metal chlorides were added and the mixture was carefully taken to dryness. The powder was rapidly transferred to a quartz tube and pumped under vacuum for 2 days at 400 °C. Finally, the tube was sealed and passed through a Bridgman furnace at 850 °C. The ampoule was broken and the crystal was polished and coated with silicone vacuum grease before mounting in the cryostat. The Eu^{3+} doping concentrations were 0.5 at% or 10 at%.

2.2. Instruments

Vacuum ultraviolet spectra were measured at the National Synchrotron Radiation Research Center, Hsinchu, Taiwan. A high-flux cylindrical grating monochromator with a focal length of 6 m was used to disperse the beam line of VUV radiation. The luminescent signal was dispersed by a monochromator with focal length of 0.32 m and a grating of 1200 grooves mm^{-1} blazed at 500 nm (with reciprocal linear dispersion of 2.5 nm mm^{-1}), and detected by a photomultiplier tube in the photon-counting mode in the spectral region between 300 and 750 nm. The luminescence intensity was corrected for incident beam intensity by using a beam splitter and sodium salicylate. The excitation monochrometer has a scan limit at 350 nm and all spectra except one were scanned to the lowest wavelength of 300 nm. The equipment does not permit measurement of luminescence decay.

3. Results and discussion

3.1. Luminescence and excitation spectra of Eu^{3+}

First, we briefly mention the $4f^6$→$4f^6$ sharp line emission of Eu^{3+}. The well-documented emission of Eu^{3+} arises from the initial ^5D_J (J=0–3) multiplets to ^7F_J [34]. In addition, Kilaan et al. [35] have observed emission from the higher energy multiplet $^5H_3$ in $NaGd_{0.98}Ce_{0.01}Eu_{0.01}F_4$ at 5 K, where the relaxed CT state is above $^5H_3$, and assumed that such emission is restricted to Eu^{3+} in fluoride lattices. As previously reported by Amberger for $Cs_2NaEuCl_6$ [34], we have observed emission from $^5D_3$ to lower ^5D_J multiplets in samples of Eu^{3+}-doped Cs_2NaYCl_6, (Fig. 1(i)), but find that when impurities such as hydroxide ion and other species are present, luminescence from the upper multiplet(s) is readily quenched. An unexpected

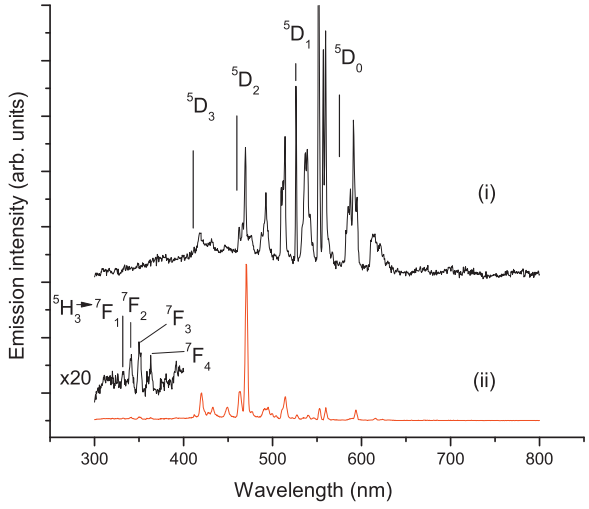

Fig. 1. (a) 10 K emission spectra of samples of (i) $Cs_2NaY_{0.9}Eu_{0.1}Cl_6$ (λ_{exc}=182.8 nm); and (ii) $Cs_2NaIn_{0.995}Eu_{0.005}Cl_6$ (λ_{exc}=266 nm). The ^5D_J luminescent states are indicated in (i) and the transitions from $^5H_3$ are shown on an expanded scale in (ii).

observation was the occurrence of emission from $^5H_3$ in $Cs_2NaInCl_6$:Eu^{3+} (Fig. 1(ii)). The lowest crystal field level, $^5H_3T_{1g}$, is located at 30,556 cm^{-1} in $Cs_2NaEuCl_6$ [36]. The gap of ~1850 cm^{-1} (7 phonons) below it to the next-lowest level ensures that non-radiative processes are sufficiently slow.

The presence of impurities is apparent from the 10 K excitation spectra of these materials. For pure $Cs_2NaEuCl_6$, the excitation spectra of the $^5D_1$ or $^5D_0$ emission exhibit bands at 240–250 nm and 262–267 nm at 10 K, with the latter at 285 nm at room temperature [2]. Whereas the longer wavelength feature has been associated with Eu–Cl CT, the shorter wavelength band could correspond to a superposition of Eu–O CT and Eu^{2+} f–d absorption bands. The wavelength of the Eu–O CT band is very sensitive to the sample synthesis method, as discovered for Y_2O_3:Eu^{3+} nanoparticles, where it was located between 229 and 248 nm [29]. Banerjee and Schwartz [32] have previously assigned the excitation band at ~260 nm in the excitation spectrum of $Cs_2NaEuCl_6$ to the Eu^{2+} $4f^7$→$4f^6$5d absorption transition. The 10 K excitation spectrum of the sample Cs_2NaYCl_6:Eu^{3+} (10 at%) shows variable intensity bands at ~240, 262, 277 nm. The excitation spectrum of $Cs_2NaInCl_6$:Eu^{3+} (0.5 at%) also exhibits impurity bands, Fig. 2. When monitoring the $^5D_2$ (514.5 nm) or $^5D_0$ (593.5 nm) emissions of Eu^{3+}, the Eu–Cl CT band is observed at 285 ± 3 nm. However, additional bands at 234, 267 nm are apparent when monitoring emission at 470.5 nm. As mentioned above, these bands could be due to Eu–O CT and/or Eu^{2+} f–d absorption transitions.

3.2. Luminescence and excitation spectra of Eu^{2+}

Fig. 3 shows the 10 K emission spectra of various hexachloroelpasolites doped with Eu^{3+}, using excitation wavelengths between 242 and 262 nm, which is well below the band gap. In each case, an emission band is observed between 412 and 444 nm. In several cases, the broad bands in Fig. 3 are decorated at lower energy by sharp, weaker features due to $^5D_2$→^7F_J transitions of Eu^{3+}. The emission band is considerably narrower for the $Cs_2NaLuCl_6$ and Cs_2NaYCl_6 host lattices (FWHM 11, 13 nm, respectively) than for Rb_2LiMCl_6 (M=Sc, 27 nm; M=Y, 33 nm). We assign these bands to trace Eu^{2+} impurity in the crystals. van Loef et al. [25] reported an emission band at 443 nm for pure Cs_2LiYCl_6, without assignment. We now propose that it is also due to trace Eu^{2+} impurity. These emission bands correspond to the $4f^6 5d^1$→$4f^7$

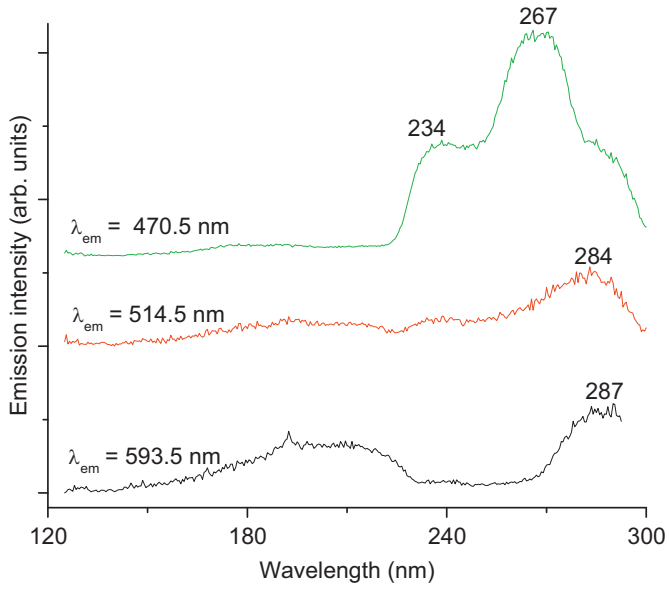

Fig. 2. 10 K excitation spectrum of $Cs_2NaInCl_6$-doped with 0.5 at% Eu at the emission wavelengths indicated.

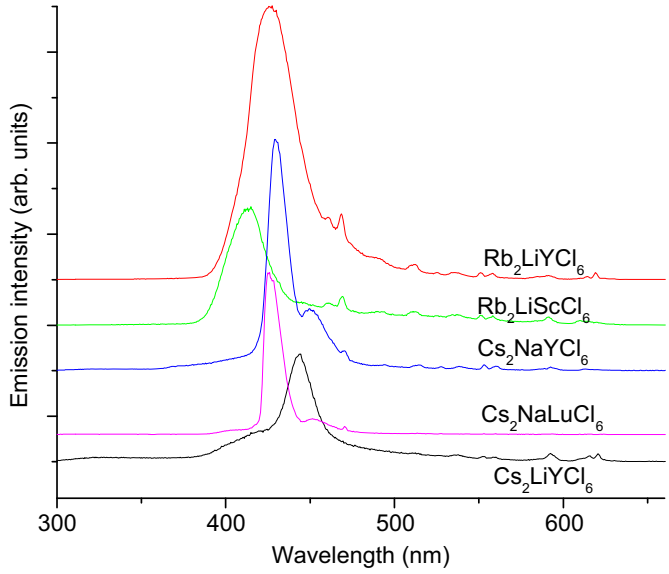

Fig. 3. 10 K emission spectra of $Cs_2NaLuCl_6$ (λ_{exc}=242 nm), Cs_2NaYCl_6 (λ_{exc}=242.5 nm), $Rb_2LiScCl_6$ (λ_{exc}=262 nm), Rb_2LiYCl_6 (λ_{exc}=262 nm), and Cs_2LiYCl_6 (λ_{exc}=261 nm) doped with 0.5% Eu^{3+} between 300 and 660 nm.

transition of Eu^{2+}. Since f–d and d–f transitions are electric dipole allowed, whereas f–f transitions are allowed by the forced electric dipole or electric dipole vibronic mechanisms [37], the intensity of the Eu^{2+} transitions dominate by factors of up to 10^6. Thus only a minute amount of Eu^{2+} produces noticeable absorption and emission bands. Furthermore, the $4f^65d$ energy level scheme of Eu^{2+} is very extensive [38] so that the excited state is readily populated by a wide range of excitation wavelengths. The emission bands in Fig. 3 show that the first excited state $^6P_{7/2}$ of $4f^7$ Eu^{2+} is located above the lowest $4f^65d$ state, otherwise sharp line $4f^7$–$4f^7$ transitions would be present. Only one $4f^65d$ emission band is expected, and the terminal state is the almost degenerate $^8S_{7/2}$ multiplet. The emission band is fairly broad because the Eu–Cl bond distance changes considerably from the $4f^7$ ground state to the $4f^65d$ excited state, giving rise to (unresolved) vibrational progressions upon the electronic origin [38]. The Eu^{2+}(VI) radius is 0.117 nm, which is a 24% increase over that of Eu^{3+}(VI) [39]. Other variable intensity, broad emission bands are observed at ~380, 470 nm in the synchrotron radiation excited spectra of hexachloroelpasolites (cf. the emission spectra of pure Cs_2NaYCl_6 in [2] and Y_2O_3 in [29]).

The corresponding excitation spectra of the broad emission bands are displayed in Fig. 4. In each case, a broad band with a maximum between 241 and 277 nm is observed. This band, at 277 nm, is very weak in the spectrum of Cs_2NaYCl_6:Eu^{3+} and it was found be variable in intensity and wavelength, depending upon the synthesis and history of the particular sample. In general, the $4f^{N-1}5d$ configurations of lanthanide ions exhibit the similarity to the $5d^1$ configuration of Ce^{3+} in that two sets of absorption bands are observed, corresponding to transitions to E_g and T_{2g} orbitals. The spectrum of $Cs_2NaLuCl_6$-doped with Eu was recorded to a longer wavelength and the observation of the further absorption bands commencing at 334 nm supports the assignment to Eu^{2+}, and is consistent with the reported absorption spectrum of Eu^{2+} in $Cs_2NaEuCl_6$ [32].

The maximum of the Eu^{2+} emission band (in cm^{-1}) is plotted against the lattice parameter for the two Cs_2NaMCl_6 systems (M=Y, Lu) in Fig. 5. The (square) datapoint for $Cs_2NaEuCl_6$ (M=Eu) is also included, where the emission band has a maximum at 442.5 nm [32]. The linear fit of these three datapoints is shown in the figure. With increasing CF strength, 10Dq, (i.e., decreasing lattice parameter), in the MF_2 series (M=Ca, Sr, Ba), and also the alkali halides, doped with Eu^{2+}, the maximum of the emission band lies at lower energy [40]. The reverse situation is observed in Fig. 4, as shown by the linear relation, where an increasing lattice parameter [41] of the $Cs_2NaLnCl_6$ series is associated with the lower energy emission band of Eu^{2+}.

From an electron paramagnetic resonance study, Boldú et al. [42] inferred that the Eu^{2+} ion in $Cs_2NaLaCl_6$ is situated at the site of the 12-coordinate, monovalent Cs^+ cation, with a neighbouring Na^+ vacancy. The delocalization of the 5d orbital over the ligands (nephelauxetic effect) contributes a large depression of the barycenter energy of the 5d orbitals. It has been predicted [43] that the crystal-field parameter B_0^4 for cuboctahedral coordination (CN=12) is −0.5 times of that for octahedral (CN=6), and 9/16 times of that for cubic coordination (CN=8), for the case of the same bond length. Recall that the bond length dependence for crystal-field parameters B_q^k from various models is $(1/R)^{\tau_k}$ with $\tau_k > k$, and that the bond length of Eu^{2+} occupying the Cs^+ site is much longer than that of Eu^{2+} in $SrCl_2$, etc. Hence the resulting crystal-field splitting in $Cs_2NaLnCl_6$:Eu^{2+} is of the order of

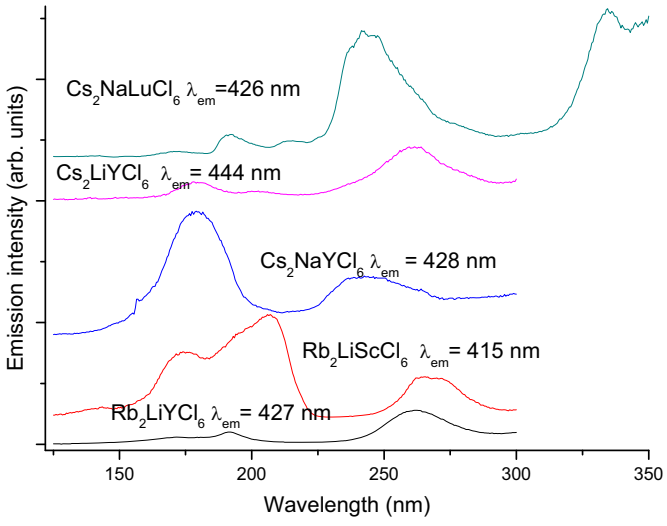

Fig. 4. 10 K excitation spectra of $M^I_2M^{II}MCl_6$ systems doped with 0.5 at% Eu. The emission wavelengths are indicated.

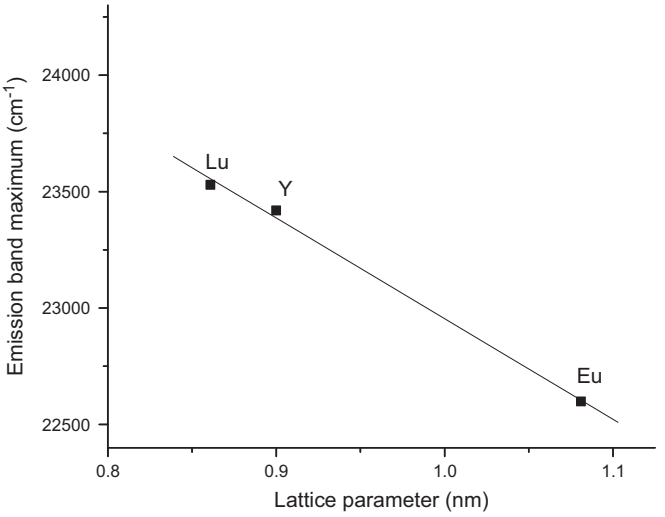

Fig. 5. Plot of Eu^{2+} emission band maximum energy and lattice parameter for Cs_2NaMCl_6 (M=Lu, Y, Eu) systems doped with 0.5 at% Eu. The linear fit is shown, with the emission band energy for Eu taken from [32].

thousands of cm^{-1}, with E_g lower than T_{2g}. Due to great mismatch between the ionic radii of Cs^+ and Eu^{2+} ions, together with the charge compensation by a univalent cation at the nearest possible position, then the distortion away from cuboctahedral (CN=12) arrangement is probably deterministic for the position of the lowest level of the Eu^{2+} 5d orbitals. Since the Cs^+–Cl^- (or Rb^+–Cl^-) distance is mainly determined by the lattice parameter, and it is much greater than the sum of the radii of Eu^{2+} and Cl^-, when the lattice constant increases, then the distortion increases, and hence the E_g orbital has a larger downshift due to the distortion. This qualitatively explains the decrease of the emission energy of Eu^{2+} with lattice parameter. The smaller ionic radius of Rb^+ (or Li^+) compared with that of Cs^+ (or Na^+), respectively, results in the deviation of the other samples from the $Cs_2NaLnCl_6$ trend.

4. Conclusions

The emission and excitation spectra of hexachloroelpasolites excited by synchrotron radiation exhibit some broad bands which are not related to $4f^N$–$4f^N$ or $4f^N$–$4f^{N-1}5d$ transitions of Ln^{3+}. Due to their deliquescent nature in air, chlorine is readily replaced by oxygen and this is shown by band between 200 and 250 nm in the excitation spectrum, which is at shorter wavelength than the Eu–Cl CT band. Other excitation bands at lower energy than 240 nm have been assigned to Eu^{2+} f–d transitions. The assignment of the corresponding Eu^{2+} emission band has been made in the spectral region between 412 and 444 nm, consistent with the previously-reported spectra of Eu^{2+} in $Cs_2NaEuCl_6$ [32]. As previously noted, it is essential to incorporate chlorine gas into the sealed tube, containing the dry product of $Cs_2NaLnCl_6$-doped with Eu from Morss method E, which is subsequently passed through a Bridgman furnace [36]. The use of vacuum, as in the present study, leads to some europium being converted from the trivalent to the divalent state.

Acknowledgements

Financial assistance from the NSFC Grant No. 11004177 is gratefully acknowledged by GJ.

References

[1] C.-K. Duan, P.A. Tanner, A. Meijerink, V. Babin, J. Phys. Condens. Matter 21 (2009) 395501.
[2] P.A. Tanner, C.-K. Duan, B.-M. Cheng, Spectrosc. Lett. 43 (2010) 431.
[3] P.A. Tanner, C.S.K. Mak, M.D. Faucher, W.M. Kwok, D.L. Phillips, V. Mikhailik, Phys. Rev. B 67 (2003) 115102.
[4] P.A. Tanner, C.S.K. Mak, N.M. Edelstein, K.M. Murdoch, G. Liu, J. Huang, L. Seijo, Z. Barandiaràn, J. Am. Chem. Soc. 125 (2003) 13225.
[5] P.S. Peijzel, P. Vergeer, A. Meijerink, M.F. Reid, L.A. Boatner, G.W. Burdick, Phys. Rev. B 71 (2005) 045116.
[6] L. van Pieterson, R.T. Wegh, A. Meijerink, M.F. Reid, J. Chem. Phys. 115 (2001) 9382.
[7] W. Ryba-Romanowski, P. Solarz, G. Dominiak-Dzik, M. Gusowski, Opt. Mater. 28 (2006) 77.
[8] V.N. Makhov, N.M. Khaidukov, N.Yu. Kirikova, M. Kirm, J.C. Krupa, T.V. Ouvarova, G. Zimmerer, Nucl. Instrum. Methods Phys. Res., Sect. A 470 (2001) 290.
[9] A.N. Belsky, J.C. Krupa, Displays 19 (1999) 185.
[10] A.J. Wojtowicz, A. Lempicki, D. Wisniewski, M. Balcerzyk, C. Brecher, IEEE Trans. Nucl. Sci. 43 (1996) 2168.
[11] M. Godlewski, K. Swiatek, A. Suchocki, J.M. Langer, J. Lumin. 48&49 (1991) 23.
[12] A. Lushchik, C. Lushchik, A. Kotlov, I. Kudryavtseva, A. Maaroos, V. Nagirnyi, E. Vasil'chenko, Radiat. Meas. 38 (2004) 747.
[13] M. Grinberg, S. Mahlik, J. Non-Cryst. Solids 354 (2008) 4163.
[14] M. Ikezawa, T. Kojima, J. Phys. Soc. Jpn. 27 (1969) 1551.
[15] D.M. Roessler, W.C. Walker, Phys. Rev. 166 (1968) 599.
[16] K. Tanimura, N. Itoh, T. Hayashi, H. Nishimura, J. Phys. Soc. Jpn. 61 (1992) 1366.
[17] Th. Pawlik, J.-M. Spaeth, Phys. Status Solidi B 203 (1997) 43.
[18] Th. Pawlik, J.-M. Spaeth, J. Phys. Condens. Matter 9 (1997) 8737.
[19] A. Bessière, P. Dorenbos, C.W.E. van Eijk, K.W. Krämer, H.U. Güdel, A. Galtayries, J. Lumin. 117 (2006) 187.
[20] A. Bessière, P. Dorenbos, C.W.E. van Eijk, L. Pidol, K.W. Krämer, H.U. Güdel, J. Phys. Condens. Matter 16 (2004) 1887.
[21] P.A. Rodnyi, V.B. Mikhailik, G.B. Stryganyuk, A.S. Voloshinovskii, C.W.E. van Eijk, G.F. Zimmerer, J. Lumin. 86 (2000) 161.
[22] J.C. van't Spijker, P. Dorenbos, C.W.E. van Eijk, M.S. Wickleder, H.U. Güdel, P.A. Rodnyi, J. Lumin. 72–74 (1997) 786.
[23] C.M. Combes, P. Dorenbos, C.W.E. van Eijk, K.W. Krämer, H.U. Güdel, J. Lumin. 82 (1999) 299.
[24] A. Bessière, P. Dorenbos, C.W.E. van Eijk, K.W. Krämer, H.U. Güdel, Nucl. Instrum. Methods Phys. Res., Sect. A 537 (2005) 242.
[25] E.V.D. van Loef, P. Dorenbos, C.W.E. van Eijk, K.W. Krämer, H.U. Güdel, J. Phys. Condens. Matter 14 (2002) 8481.
[26] M.S. Alam, E. Janata, Chem. Phys. Lett. 417 (2006) 363.
[27] T. Andersen, J.L. Baptista, Phys. Status Solidi B 44 (1971) 29.
[28] F. Fischer, H. Gründig, R. Hilsch, Z. Phys. 189 (1966) 79.
[29] P.A. Tanner, L. Fu, B.-M. Cheng, J. Phys. Chem. C 113 (2009) 10773.
[30] L. van Pieterson, M. Heeroma, E. de Heer, A. Meijerink, J. Lumin. 91 (2000) 177.
[31] J.L. Ryan, C.K. Jørgensen, J. Phys. Chem. 70 (1966) 2845.
[32] A.K. Banerjee, R.W Schwartz, J. Phys. Chem. Solids 42 (1981) 1057.
[33] L.R. Morss, M. Siegal, L. Stenger, N. Edelstein, Inorg. Chem. 9 (1970) 1771.
[34] H.-D. Amberger, Z. Phys. Chem. 109 (1978) 125.
[35] H.S. Kiliaan, J.F.A.K. Kotte, G. Blasse, Chem. Phys. Lett. 133 (1987) 425.
[36] J.R.G. Thorne, M. Jones, C.S. McCaw, K.M. Murdoch, R.G. Denning, N.M. Khaidukov, J. Phys. Condens. Matter 11 (1999) 7851.
[37] P.A. Tanner, C.-K. Duan, Coord. Chem. Rev. 254 (2010) 3026.
[38] Z. Pan, L. Ning, B.-M. Cheng, P.A. Tanner, Chem. Phys. Lett. 428 (2006) 78.
[39] R.D. Shannon, Acta Crystallogr. A32 (1976) 751.
[40] J. Rubio O, J. Phys. Chem. Solids 52 (1991) 101.
[41] G. Meyer, Prog. Solid State Chem. 14 (1982) 141.
[42] J.L. Boldú, R.J. Gleason, C. Quintanar, E. Munoz, J. Phys. Chem. Solids 57 (1996) 267.
[43] C. Görller-Walrand, K. Binnemans, in: K.A. Gschneidner Jr., L. Eyring (Eds.), Handbook on the Physics and Chemistry of Rare Earths, Elsevier Science B.V, Amsterdam, 1996, pp. 121–283. Chapter 23.